Experimental and computational evaluation of area selectively immobilized horseradish peroxidase in a microfluidic device

Hoffmann, Christian; Pereira Rosinha Grundtvig, Ines; Thrane, Joachim; Garg, Nipun; Gernaey, Krist V.; Pinelo, Manuel; Woodley, John; Krühne, Ulrich; Daugaard, Anders Egede

Published in:
Chemical Engineering Journal

Link to article, DOI:
10.1016/j.cej.2017.09.050

Publication date:
2017

Document Version
Peer reviewed version

Accepted Manuscript

Experimental and computational evaluation of area selectively immobilized horseradish peroxidase in a microfluidic device

Christian Hoffmann, Inês P. Rosinha Grundtvig, Joachim Thrane, Nipun Garg, Krist V. Gernaey, Manuel Pinelo, John M. Woodley, Ulrich Krühne, Anders E. Daugaard

PII: S1385-8947(17)31548-6
DOI: http://dx.doi.org/10.1016/j.cej.2017.09.050
Reference: CEJ 17635

To appear in: *Chemical Engineering Journal*

Received Date: 20 April 2017
Revised Date: 11 August 2017
Accepted Date: 7 September 2017

Please cite this article as: C. Hoffmann, I.P. Rosinha Grundtvig, J. Thrane, N. Garg, K.V. Gernaey, M. Pinelo, J.M. Woodley, U. Krühne, A.E. Daugaard, Experimental and computational evaluation of area selectively immobilized horseradish peroxidase in a microfluidic device, *Chemical Engineering Journal* (2017), doi: http://dx.doi.org/10.1016/j.cej.2017.09.050

Experimental and computational evaluation of area selectively immobilized horseradish peroxidase in a microfluidic device

Christian Hoffmann[a], Inês P. Rosinha Grundtvig[b], Joachim Thrane[b], Nipun Garg[a], Krist V. Gernaey[b], Manuel Pinelo[c], John M. Woodley[b], Ulrich Krühne[b], Anders E. Daugaard[a,*]

[a]Danish Polymer Centre, Department of Chemical and Biochemical Engineering, Technical University of Denmark, Søltofts Plads Building 229, 2800 Kgs. Lyngby, Denmark

[b]Process and Systems Engineering Center (PROSYS), Department of Chemical and Biochemical Engineering, Technical University of Denmark, Søltofts Plads Building 229, 2800 Kgs. Lyngby, Denmark

[c]Center for BioProcess Engineering, Department of Chemical and Biochemical Engineering, Technical University of Denmark, Søltofts Plads Building 229, 2800 Kgs. Lyngby, Denmark

*Corresponding author, adt@kt.dtu.dk

Abstract

A microreactor with a square shaped reactor chamber was developed with the aim to correlate enzyme positioning with biocatalytic activity. The enzyme position as an important parameter to improve the contribution of the individual enzymes towards the overall reactor efficacy was therefore evaluated experimentally and by computational fluid dynamics (CFD) simulations. Ultimately, such a correlation would lead to faster development through computational pre-screening and optimized experimental design.

In this proof-of-concept study, microreactors were prepared in a 2-step curing process of an off-stoichiometric thiol-ene-epoxy (OSTE+) mixture employing both a thiol-ene (TEC) and a thiol-epoxy curing reaction. Subsequent surface functionalization of the remaining thiol groups on the reactor surface through stenciled photoinitiated TEC enabled the preparation of specific surface patterns in the reactor. Patterns were visualized using an allyl-functional disperse red dye, illustrating the successful preparation of a fully reacted surface, a half covered surface and 2 checkerboard patterns. Similarly, allyl glycidyl ether was exploited to functionalize the microreactor surface with epoxide groups, which were used for covalent immobilization of horseradish peroxidase (HRP) in the same patterns. Biocatalytic activity measurements confirmed a clear dependency of the overall reactor performance depending on the spatial distribution of the immobilized enzymes, where specifically the two checkerboard motifs were identified as being particularly effective compared to enzymes covering homogeneously the entire reactor surface. The performance of the same configurations was additionally determined by 3-dimensional CFD simulations. The computational model predicted the same tendencies for the overall reactor performance as obtained from experimental determination. This good agreement between the obtained experimental and computational results confirmed the high potential of CFD models for predicting and optimizing the biocatalytic performance of such a reactor.

Keywords

Microfluidics; thiol-ene chemistry; enzyme immobilization; surface functionalization; computational fluid dynamic simulation (CFD)

1. Introduction

The application of enzymes as biocatalysts in industrial processes has attracted increased attention in recent years due to several major advantages of enzymes compared to conventional catalysts. Enzymes originate from renewable resources and take part in green processes with a high catalytic selectivity under mild reaction conditions [1]. These advantageous properties make them attractive for specific applications like synthesis of targeted enantiomerically-pure chiral compounds relevant for pharmaceuticals. However, the disadvantage of enzymes for application at large scale and in continuous processes is their low long-term stability. In order to increase the attractiveness of enzymes for industrial processes, improving their long-term biocatalytic efficiency is a key target. It is well known that an increase in enzyme stability, and consequently biocatalytic productivity, can be achieved through immobilization on solid supports [2–4]. In particular, polymers have shown high potential as enzyme carriers generating biocatalytic systems with an improved stability to external conditions, such as temperature, pH and reaction media [5]. The binding of enzymes on support surfaces can generally be established by adsorption, ionic or covalent bond formation. However, the positive effect in terms of stability is frequently offset by a loss in biocatalytic activity. One explanation is the decreased accessibility to the enzyme's active site by the substrate due to conformational restrictions by attaching the protein to the support material. In order to overcome this, the preservation of the natural environment for a specific enzyme has been identified to be of high importance [6]. This can be realized by chemical modification of the surface, such as by increasing the hydrophilicity of the surface. Functionalization with poly(ethylene glycol) (PEG) for instance shows an improvement in enzymatic activity [7]. Developments in reactor design and reaction conditions play an additional role in order to optimize enzyme efficiency and consequently entire biocatalytic processes. We recently reported that biocatalytic reactors with immobilized enzymes can exhibit differences in their overall productivity, depending on the local position of the enzymes within the flow field of the reactor [8]. Changing the surface pattern of a given amount of enzyme resulted in a different productivity. It was shown that optimization of the spatial distribution of the immobilized enzymes could thus lead to an improved reactor efficiency.

In order to test the influence of such modifications in continuous flow systems, microfluidic devices have been proven to be suitable due to their small size, low consumption of reagents and limited reaction volumes as well as high throughput combined with a high degree of reproducibility [9,10]. Additionally, good heat and mass transfer in combination with laminar flow provide good control over reaction conditions [11]. Laminar flow restricts mixing to occur exclusively by diffusion, unless this is circumvented by specific microchannel configurations.

Heterogeneous reactions take place solely on the surface of the catalyst or on the surface that the catalyst is bound to. In these systems, diffusion shows a great impact on the overall reaction, which is influenced by many different parameters, such as flow rate, concentration, dimensions of the reactor geometry and reaction rate [12]. Microfluidic systems are traditionally fabricated in glass or polymeric materials such as poly(methyl methacrylate) (PMMA) or poly(dimethylsiloxane) (PDMS) [13–15]. Especially PDMS has been used extensively for microfluidics due to the ease of fabrication and relatively low cost [16]. Mold casting enables the preparation of different reactor designs and has been applied for the development of biocatalytic microreactors. Hence, enzymes were immobilized on polymer microbeads [17,18] or onto the reactor walls [19]. Alternatively, the formation of a surface patterned phospholipid bi-layer or an adsorbed protein layer [20] enabled the attachment of enzymes on the PDMS surfaces.

Direct protein and enzyme immobilization onto polymer surfaces in microfluidic devices in off-stoichiometric thiol-ene (OSTE) material is an interesting alternative to the currently used PDMS systems. OSTE thermosets have recently evolved into a very versatile platform, which have been successfully applied for fabrication of microfluidic devices [21]. Generally, OSTE systems consist of a multifunctional thiol and a multifunctional alkene (ene) reacting through thiol-ene chemistry (TEC) either under photochemical or thermal conditions [22]. OSTE networks are compatible with many organic solvents, are thermally stable and can be directly surface functionalized. Material properties can be controlled by selecting from a large variety of reagents, which makes this system very versatile. The OSTE approach has recently been updated in order to improve mechanical properties as well as surface bonding, which is essential for the fabrication of microfluidics. In this OSTE+ system, Bisphenol A diglycidyl ether (BADC) undergoes a thiol-epoxy reaction in an additional, orthogonal curing step. This enables covalent sealing between interfaces of the precured material in order to prevent leaking under operating conditions, which is a well-known challenge in microfluidics [23,24]. Mechanical properties of the thermoset can be controlled by stoichiometric variations between thiol and ene groups. Furthermore, off-stoichiometric ratios result in excess of unreacted functional groups, either thiol or ene [25]. These functional groups are well suited for further surface functionalization via photochemical TEC, which has been applied for tailoring surface properties [26,27] or introducing different functional molecules [28]. Additionally, photochemical TEC on the surface offers a possible pathway for surface modification in various patterns by application of a stencil [29,30].

So far, OSTE(+) thermosets have been rarely used for the immobilization of enzymes. Lafleur and coworkers utilized OSTE monoliths for the immobilization of galactose oxidase and peptide-N-glycosidase F after surface activation by means of L-ascorbic acid linking groups [31].

The performance of biocatalytic reactors can generally be improved by different approaches, such as the optimization of reactor architecture and geometries. Recently, Schäpper et al. developed a theoretical topology optimization of immobilization of yeast cells, which resulted in an 8-10 fold improvement in theoretical production rate [32]. Inspired by this approach and by applying isolated enzymes instead of whole cells, we demonstrated using computational fluid dynamic (CFD) simulations that in a laminar flow field of a square reactor with a distributed flow pattern, the biocatalytic reactor efficacy considerably depends on the positioning of the immobilized enzyme [8]. By varying computationally the topology of immobilized enzymes inside the microreactor, simulated reactor configurations with substantially improved productivities were obtained. To the best of our knowledge, reactor optimization based on the positioning of the immobilized biocatalyst within the reactor, either computationally or experimentally, has not yet been done.

The objective of this proof-of-concept study was the methodological development of a biocatalytic reactor, which enabled experimental and computational investigation of the effect of the local distribution of immobilized enzymes towards the overall reactor efficacy. The correlation between experimental and computational results should demonstrate the potential of CFD simulations to predict the biocatalytic performance of such reactors, and would thus open up for the use of CFD for optimization of the microfluidic reactor configuration. In order to achieve this, an enzymatic microreactor containing immobilized horseradish peroxidase as a model enzyme in distinct surface patterns was developed. A square reactor geometry was selected in order to achieve a specific flow pattern characterized by a velocity distribution across the reactor. The laminar flow within the reactor made it possible to assess the impact of selectively distributing the immobilized enzyme on the overall reactor productivity. The impact of the spatial distribution of surface immobilized HRP towards the biocatalytic performance was determined and the results were correlated to those obtained from CFD simulations. This strategy offers a possibility for reactor development and can facilitate the optimization process of new catalytic reactors.

2. Experimental

2.1. Materials

Pentaerythritol tetrakis(3-mercaptopropionate) (PETMP, >95%), 1,3,5-Triallyl-1,3,5-triazine-2,4,6(1H,3H,5H)-trione (TATATO, 98%), bisphenol A diglycidyl ether (BADC, >95%), 1,5-Diazabicyclo[4.3.0]non-5-ene (DBN), allyl bromide (97%), disperse red 1 (95%), potassium hydroxide, 18-crown-6-ether, allyl glycidyl ether (>99%), horseradish peroxidase (HRP, lyophilized powder, 50-150 U mg^{-1}), 2,2′-Azino-bis(3-ethylbenzothiazoline-6-sulfonic acid) diammonium salt (ABTS, ≥98%), hydrogen peroxide (3%), toluene and THF were obtained from Sigma Aldrich and used without further purification. Lucirin TPO-L (ethyl-2, 4, 6-tri- methylbenzoylphenyl phosphinate) was purchased from BASF. Sylgard 184 – poly(dimethylsiloxane) (PDMS) elastomer kit was purchased from Dow Corning.

2.2. Characterization

NMR spectroscopy was carried out on a Bruker Avance 300 MHz spectrometer. Chemical shifts are given in ppm.

2.3. Microchip preparation

Master molds for the top and bottom part of the microfluidic device fabricated in poly(methyl methacrylate) (PMMA) were micro-milled in order to use them for the preparation of negative molds. Those were prepared from PDMS (Sylgard 184 elastomer kit) by curing at 80 °C and casting from the master molds. The PDMS molds were utilized for all further microchip preparation procedures. For this in brief, PETMP, TATATO and BADC were mixed in a functionality ratio of 2.0 : 1.0 : 0.25. Lucirin (1.0 wt%) and DBN (1.0 wt%) were added and the solution was homogenized by mixing in a Speedmixer (SpeedMixer™ DAC 150.1 FVZ) for 2 min at 3000 rpm and subsequently poured into the PDMS molds and covered with a PMMA slide (thickness 2 mm) in order to ensure uniform thickness. In the subsequent light induced curing step, this mixture was irradiated with UV light (= 365 nm, 2.9 mW cm^{-2} without and 1.6 mW cm^{-2} with PMMA slide on top of the thiol-ene mixture) for 10 min. The obtained upper and lower layer of the microchip were aligned and properly attached to each other. Two thin PMMA plates, one on top and one at the bottom, were fixed at the microchip and by employing several clamps; the system was mechanically sealed in order to provide best contact. Subsequently, the microchip was thermally cured at 80 °C under vacuum for 2 h. The resulting sealed microchips were used without further treatment.

2.4. Synthesis of allyl disperse red 1

18-crown-6-ether (12.9 mg, 0.048 mmol), THF/water (10 mL, 99.5:0.5 vol%), potassium hydroxide (0.693 g, 12.1 mmol) and disperse red 1 (1.00 g, 3.03 mmol) were added into a round bottom flask and stirred at room temperature for 1 h. Allyl bromide (0.81 mL, 9.08 mmol) was subsequently added at room temperature. The solution was stirred for 21 h until the substrate was fully converted, which was determined by thin layer chromatography in heptane/ethyl acetate (60:40). After addition of ammonium chloride solution (NH_4Cl, 20 mL, 2 M), the reaction solution was extracted with dichloromethane (5x20 mL). The organic phase was dried over $MgSO_4$, filtrated and subsequently concentrated in vacuo leading to a dark red solid powder as the final product (1.18 g, 86 % yield).

2.5. Microchip surface modification with allyl disperse red 1

An allyl disperse red 1 (83.8 mg, 0.30 M) solution was prepared in toluene (0.8 mL) containing benzotriazole (0.69 mM) and Lucirin (33 mM). During the entire procedure light exposure of the reaction solution was minimized by covering vials and syringes with aluminum foil. Before filling the microchip with the reactive solution, a stencil mask (with specific pattern) made of a black polypropylene (PP) sheet was attached on top of it and a black PP sheet on the bottom of the chip. Then, an aliquot of the light sensitive solution was added into the cavity of the microchip using a syringe. The microchip was then irradiated with UV light (λ= 365 nm, 1.0 mW cm^{-2}) from the top for 3 min and subsequently covered with aluminum foil and flushed continuously with 80 mL of toluene for 240 min.

2.6. Microchip surface modification for enzyme immobilization

For the surface modification, 174 µL allyl glycidyl ether (1.47 mmol, 0.29 mM) and 4.83 mL toluene (containing 0.78 mM benzotriazole) were added into a vial. During the entire procedure light exposure of the reaction solution was minimized by covering vials and syringes with aluminum foil. Subsequently, 51.6 mg of Lucirin (0.163 mmol, 33 mM) were added and the solution was homogenized by mixing using a Vortex mixer. Before filling the microchip with the reactive solution, a black polypropylene (PP) stencil mask (with specific pattern) was attached on top of it. Additionally, the bottom of the chip was also covered with a black PP mask. Then, an aliquot of the light sensitive solution was added into the cavity of the microchip using a syringe. The microchip was then irradiated with UV light (λ= 365 nm, 1.0 mW cm^{-2}) from the top for 3 min and subsequently covered with

aluminum foil and flushed continuously with 50 mL of toluene for 180 min. The solvent was evaporated in a vacuum oven at room temperature.

2.7. Horseradish peroxidase immobilization

The surface modified microchips were filled with HRP solution (1.0 mg mL^{-1} in PBS buffer pH 7.2) and incubated for 15 h at 4 °C. Then, the supernatant immobilization solution was removed and the microchip was flushed with 25 mL of PBS buffer (pH 7.2) within 1 h.

2.8. Activity study

The microchip was filled with phosphate buffer (0.1 M, pH 5). Subsequently the inlet of the microchip was attached to a syringe pump and the outlet to a UV-Vis detector for online absorbance measurements [33]. The microchip was continuously flushed with phosphate buffer solution (0.1M, pH5) containing ABTS (1.0 mM) and hydrogen peroxide (2.0 mM) at a flow rate of 225 µL min^{-1}.using a syringe pump (500µL, Tecan Cavro XLP6000) The outlet of the microreactor was connected to an 8-port injection valve (VICIE45-230-CR2 head) which was programmed to collect samples every 16s. The UV-Vis detector (Agilent G1315AR) recorded the absorbance at wavelengths of 340 and 414 nm corresponding to the absorbance maxima of the substrate (ABTS) and its oxidized product ($ABTS^{\bullet+}$), respectively. After reaching steady state conditions, the measurements were constantly recorded for a further 30 min. Afterwards the microchips were rinsed with phosphate (0.1 M, pH 5) and PBS buffer (pH 7.4). A schematic drawing of the setup can be found in the supporting information (SI-Fig. 1).

2.9. Computational fluid dynamic simulation

Each microreactor geometry was designed and discretized in calculation elements using the software ICEM CFD® 16.0. The number of elements for the four simulated structures varied between 850000 and 900000 elements. The setup of the system as well as the 3-dimensional simulations were performed with help of the commercial software ANSYS CFX (16.0). The flow inside was simulated as a steady state laminar flow, with a constant flow rate of 225 µL min^{-1} matching the experimental conditions. The diffusion coefficients used in the computational investigation have been previously reported in the scientific literature [34]. The diffusion coefficients for both the substrate and the product were assumed to be the same, $2.4 \cdot 10^{-10}$ m^2 s^{-1}, since there are no significant structural changes for the

molecules. The kinetic parameters K_M and k_{cat} were experimentally determined by maintaining the hydrogen peroxide concentration constant, which simplifies the Ping Pong Bi Bi kinetic mechanism to the Michaelis-Menten mechanism. The apparent kinetic parameters were determined from this mechanism. The Michaelis-Menten constant (K_M) and the maximum reaction rate (V_{max}) were calculated using the Hanes-Wolf method and the turnover number (k_{cat}) was obtained through the linear relation between the V_{max} values and the enzyme concentration. The experimentally determined reaction kinetic parameters are: k_{cat} = 732 s^{-1} and K_M = 0.76 mM. The immobilized enzyme is defined as a wall on which the reaction occurs. The enzyme concentration on the surface was determined considering that the diameter of an enzyme molecule is assumed to be roughly 10 nm. From the area of a molecule ($7.85 \cdot 10^{-17}$ m^2), the maximum concentration of enzyme that can be immobilized in a monolayer is calculated as $2.12 \cdot 10^{-8}$ $mol \cdot m^{-2}$ [35]. The dimensions of the immobilization areas in the CFD simulation are the same as the areas of the experimental work.

The performance of each structure was evaluated by considering the average product concentration at the outlet at steady state as the performance indicator.

3. Results and discussion

In Figure 1 the fabrication process of the thiol-ene-epoxy based microreactors is illustrated, including the used monomers (A), the photochemical (B) and the subsequent thermal (C) curing step. As base compounds PETMP, TATATO and BADC (see Figure 1A) were used in a ratio of 2.0:1.0:0.25.

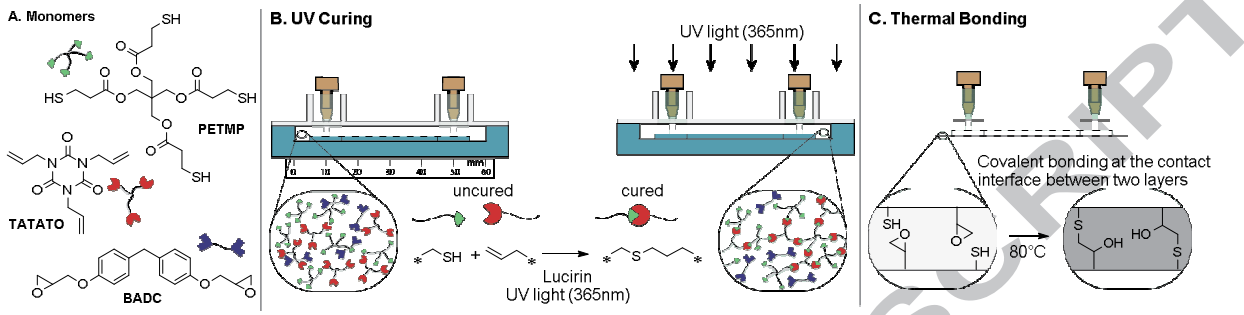

Figure 1. Schematic representation of the preparation of OSTE+ microchips with subsequent surface modification. A) Monomers for OSTE+ preparation tetra functional thiol PETMP, trifunctional allyl TATATO and bifunctional BADC, B) First UV curing of the OSTE+ mixture via thiol-ene reaction followed by C) a second curing that seals the system "leakage free"

The liquid mixture was cured in a PDMS mold using lucirin as a photoinitiator and UV light (λ=365 nm), as illustrated in Figure 1B. After crosslinking, the upper and lower part of the microchip were assembled and residual epoxide and thiol groups were utilized in a thermal bonding reaction at the interface, which resulted in a stable and leakage-free microreactor (see Figure 1C). The geometry of the microreactor is based on a square shape with a length and width of 30 mm and a thickness of 0.25 mm with an inlet and outlet channel of 10 mm in length and width located at the two opposite ends of the reactor, as can be seen in Figure 2A.

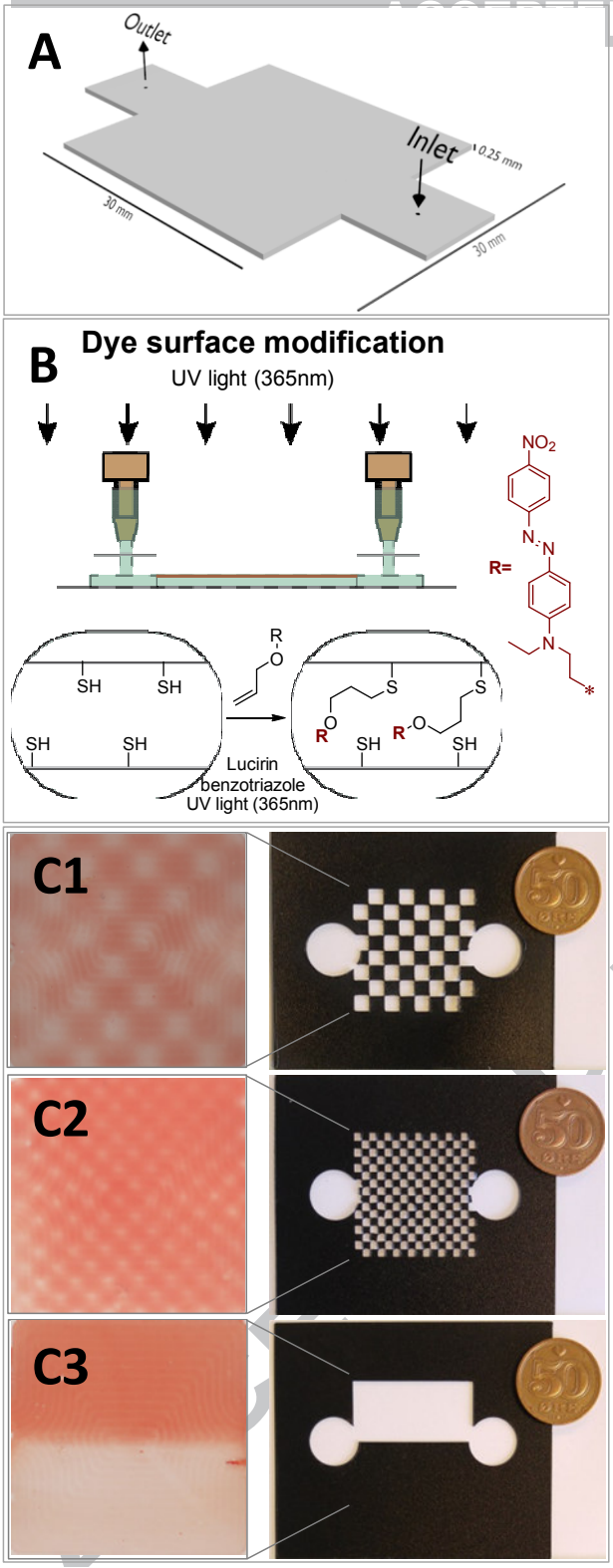

Figure 2. A) Microreactor geometry, B) Microreactor surface modification via TEC using allyl disperse red, C1-3) Images of surface functionalized microchips using allyl disperse red and different stencil masks: C1 – coarse checkerboard, C2 – fine checkerboard, C3 - half reacted surface

The reactor was prepared using a thiol-ene mixture with excess of PETMP, which leads to residual unreacted thiol groups within the bulk material and on the reactor surface. These free thiol groups on the microreactor surface permit functionalization of the surface after assembly of the microfluidic system. Application of stencil masks combined with UV initiated surface grafting enabled preparation of various patterns in the reactor. In order to test the enzymatic activity of immobilized enzymes in various configurations, four different geometric patterns were selected. A full surface (30 x 30 mm^2), a half surface (15 x 30 mm^2) and two checkerboard patterns with either a fine (256 squares of 1.7 x 1.7 mm^2 each of which 128 were modified) or a coarse (64 squares of 3.55 x 3.55 mm^2 each of which 32 were modified) were prepared. In order to test and visualize the surface patterning, an allyl functional disperse red dye was used as shown schematically in Figure 2B. The high selectivity of the reaction permits direct and accurate replication of the applied stencils as shown in the photographs of the final surfaces in Figure 2C. Additionally, due to the use of benzotriazole as UV-absorber, significant reaction selectivity for the irradiated surface was obtained. In fact, by irradiation from the top, exclusively the upper surface of the reactor cavity was modified with the allyl disperse red leaving the bottom surface unreacted. An image of the upper and lower surface after photochemical reaction with the red dye can be found in the supporting information (SI-Fig. 2). The surface modification procedure offers a controlled area functionalization with high selectivity for the irradiated surface by UV initiated TEC. Replacement of the dye with allyl glycidyl ether undergoing the same TEC leads to surface patterned epoxides, which are known to covalently bind enzymes via ring-opening with free amine residues from the enzyme structure [36]. The reaction scheme from surface modification with allyl glycidyl ether and subsequent covalent immobilization of horseradish peroxidase (HRP, EC 1.11.1.7) can be seen in Figure 3.

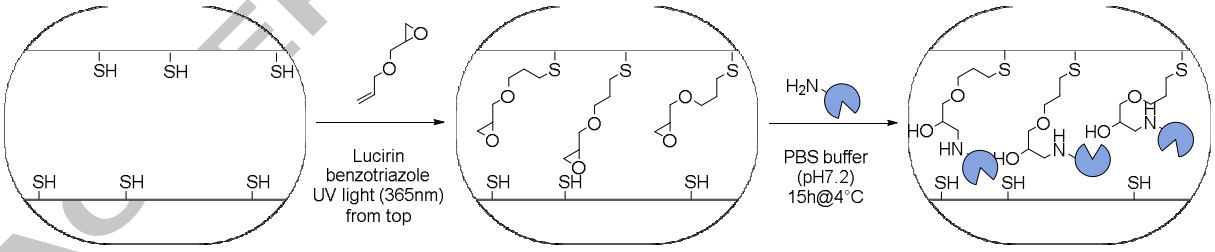

Figure 3. Microchip functionalization of remaining surface thiol groups using allyl glycidyl ether via UV initiated thiol-ene reaction and subsequent covalent HRP immobilization with introduced epoxide groups on the microreactor surface

HRP dissolved in PBS buffer was immobilized on the epoxy patterned reactors by overnight incubation. HRP is a well-studied enzyme, which oxidizes a wide range of aromatic compounds in the presence of hydrogen peroxide (H_2O_2). It can be widely applied in bio-sensing, medical diagnostics and other biomedical applications [37,38]. The quantification of the immobilized amount of HRP was attempted using the Bradford assay [39] and the bicinchoninic acid (BCA) assay, which were in both cases inconclusive due to the low concentration of enzyme and interference with residual thiol groups on the surface, respectively [40]. Quantification using fluorescently labeled enzymes on thiol-ene surfaces confirmed the presence of immobilized enzymes on the surface, but could not be used to determine the amount of attached enzyme due to background fluorescence from the material (see SI-Fig. 3). Therefore, the exact quantification of the enzyme concentration on the surfaces is not possible.

In the presence of H_2O_2, HRP catalyzes a one-electron oxidation of 2,2′-azino-bis(3-ethylbenzothiazoline-6-sulfonate) (ABTS) to a radical cationic product ($ABTS^{\bullet+}$). The absorbance maximum of ABTS at 340 nm (ε_{340}=3.6 x 10^4 M^{-1} cm^{-1}) is shifted to 414 nm (ε_{414}=3.6 x 10^4 M^{-1} cm^{-1}) for its oxidized product $ABTS^{\bullet+}$, from which the activity of immobilized HRP can be determined [41]. Kinetic parameters of immobilized HRP have been studied previously in a microfluidic packed bed reactor [18], monolith structures [42] or on planar surfaces [43]. It has been shown that apparent enzyme kinetics vary greatly depending on the applied configuration, flow rate and type of immobilization compared to that of enzymes free in solution. In this study, HRP was uniformly immobilized via covalent bonding on the same support, which resulted in the same individual activity for all immobilized enzymes. However, their contribution to the overall reactor activity is a function of many parameters, including flow rate mass transfer, diffusion but also the spatial distribution of the immobilized enzymes in the microreactor. The used concentrations of ABTS and H_2O_2 were significantly higher than required for the applied conditions in order to ensure large excess of substrates. The overall reactor performance of the individual configurations was constantly measured over time as shown in SI-Figure 4. An average of the absorbance measured under steady state conditions between 350 and 850 s, which was in agreement with CFD, correlated directly to the formed product at the outlet of the reactor, as presented in Figure 4.

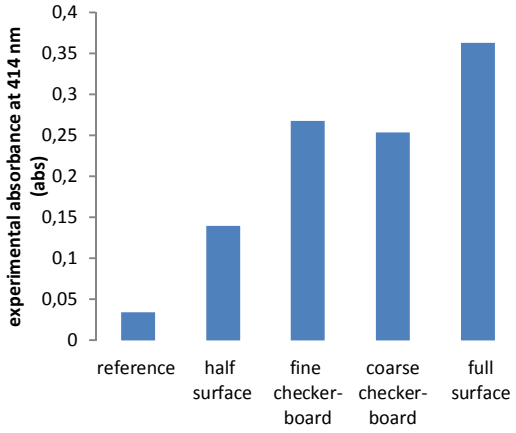

Figure 4. Overall reactor performance of the different reactor configurations illustrated as absorbance measurements at 414 nm corresponding to the formed product at the reactor outlet

A reference measurement was performed, in order to eliminate the potential contribution of adsorbed enzymes to the measured activities. This native surface, undergoing the same enzyme incubation procedure, did not show any activity (Figure 4, reference). Therefore the absence of unspecific adsorption of HRP on the selected surfaces could be confirmed, which makes this surface well suited for immobilization of HRP. These results of the four different configurations show clearly that the fully modified microreactor, containing the largest activated surface and thus the highest amount of immobilized HRP, was the most active one. The two checkerboard structures had a reduced performance by 26 and 30 % of that of the fully immobilized surface. Furthermore, the overall reactor activity was reduced even further when only half of the reactor surface was modified.

The main focus of this study was the determination of the effect of enzyme distribution over the reactor surface and the specific system was therefore designed only to illustrate the impact of different surface patterns. Therefore, the product absorbance for the individual patterns is additionally shown relative to the respective modified surface area, which allows direct comparison of the reactor efficiency between the selected patterns (see Figure 5A). The areas of the individual activated surface patterns were calculated from the applied photomasks (see SI-Table 1).

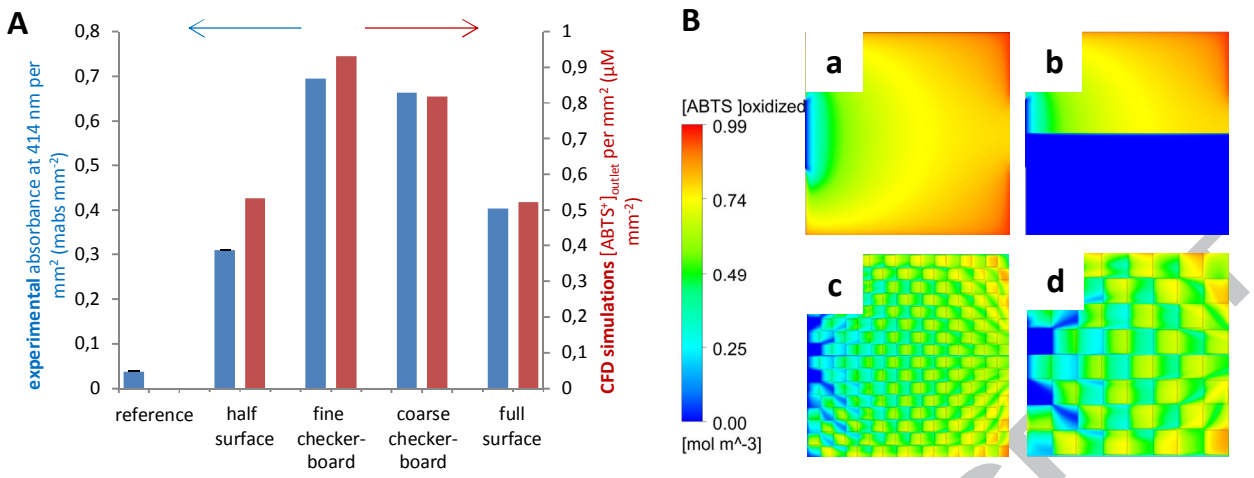

Figure 5. Comparison of experimentally determined $ABTS^{\bullet+}$ absorbance at 414 nm per mm^2 modified area at the reactor outlet in steady state condition (blue) and $ABTS^{\bullet+}$ outlet concentration obtained from CFD simulations in mM mm^{-2} (red) of various surface patterns, reference (HRP adsorption on non-modified surface, empty squares), half modified surface, coarse checkerboard, fine checkerboard, fully modified surface; and B) Illustration of product concentration on the top surface in the microreactor (in steady state simulations) dimensions using fully modified surface (a), half modified surface (b), fine checkerboard structure (c), coarse checkerboard structure (d), where red surfaces illustrate a high and blue surfaces a low product concentration.

Investigating the impact of different patterns demonstrated a slightly reduced absorbance per enzyme area (by 23%) for the microreactor with half of the area covered compared to the fully modified surface, which was not entirely plausible due to symmetry of the pattern, but was finally attributed to experimental inaccuracy. However, the fine and the coarse checkerboard structures exhibited an increased efficiency with 81 and 56 % higher absorbance per active area than the fully modified surface, which demonstrates a significant improvement in product concentration relative to the functionalized surface area or in other words, amount of immobilized enzyme. In fact, it is clearly demonstrated here that the enzyme distribution over the surface affects the overall activity of the microreactor. This improvement of the reactor productivity is influenced by a series of other factors such as flow conditions, substrate diffusion rates and local substrate concentrations. The flow within this reactor geometry is characterized by a gradient, in which the highest velocity is present in the center of the reactor and a reduced velocity at the sides. The difference in velocities across the reactor can consequently influence the mass transport and mixing of the fluid. Therefore, the accessibility of substrate for the enzyme near the surface depends on the

position and the local conditions. The selection of this particular reactor design was used in order to generate this complexity of overlapping phenomena.

Computational fluid dynamic (CFD) simulations were conducted in order to validate the experimentally determined performance of the microreactors as a function of the different enzyme immobilization patterns, the impact of the laminar flow conditions, geometry and material transport limitations (diffusion). The product concentrations at the outlet of the reactor for each modified surface area were determined, as presented in Figure 5A (red) and visualized in different patterns, as shown in Figure 5B.

In the flow simulations under steady-state condition all parameters were selected to reflect the experimental setup, such as dimensions of the microreactor, outlet, inlet and immobilization patterns, flow rates, substrate concentrations and theoretical diffusivity. Therefore, it is not possible to compare the results from the experimental and the computational results directly, but merely the trends. Using the same surface patterns, the CFD simulations exhibit the same trend in terms of reactor efficiency as seen in the experimental setup (see Figure 5A, red). The simulation of the full and half modified surface show very similar product concentrations relative to the activated surface area. Similarly for the experimental results, the product concentration obtained from CFD simulations showed an increase of 78 and 57 % for the fine and the coarse checkerboard structure compared to the fully modified surface. The experimental results and computational findings correlate well and demonstrate a clear dependence of the overall product formation relative to the distribution pattern of enzymes on the modified surface area.

4. Conclusions

In order to demonstrate how the position of immobilized enzymes influences the biocatalytic efficacy of a reactor and thus, how reactor performance can be predicted; we have developed a method that correlates experimental results with microreactors containing patterned immobilized enzyme surfaces to CFD simulations as a proof-of-concept study. Initially, an experimental setup was prepared in which HRP could be selectively immobilized in specific patterns onto the surface of an OSTE+ microfluidic reactor. OSTE+ based microfluidic devices were surface modified with allyl disperse red, illustrating the effect of applied stencil masks, and with allyl glycidyl ether enabling the covalent immobilization of HRP. High selectivity of the stencils and exclusive functionalization of the directly irradiated surface was achieved by use of a UV absorber. The performance of the microreactors was

significantly influenced by patterning of the enzyme on the surface and two checkerboard structures (fine and coarse patterns) showed an increased efficiency compared to a half area covered reactor, even though the total area of immobilized enzyme was similar. These results correlated very well with CFD simulations of the same reactor designs, illustrating that the configuration pattern plays a significant role in explaining the outstanding performance of the two checkerboard structures. The good agreement between experimental and computational results demonstrates the potential of computational models in order to predict and optimize the performance of such reactors. Further reactor optimization using computational simulations in combination with experimental reactor preparation is the subject of ongoing research.

Acknowledgements

The authors wish to thank the Johanne Louis-Hansens Endowment for financial support. Additionally, it is gratefully thanked for funding from the European Union FP7 (FP7/2007-2013) Project BIOINTENSE – Mastering Bioprocess integration and intensification across scales (Grant Agreement number 312148). Furthermore, Rolf Hoffmeyer Ringborg is acknowledged for support with the continuous enzyme activity measurements.

References

[1] R. DiCosimo, J. McAuliffe, A.J. Poulose, G. Bohlmann, Industrial use of immobilized enzymes, Chem. Soc. Rev. 42 (2013) 6437–74. doi:10.1039/c3cs35506c.

[2] R.A. Sheldon, S. van Pelt, Enzyme immobilisation in biocatalysis: why, what and how, Chem. Soc. Rev. 42 (2013) 6223–35. doi:10.1039/c3cs60075k.

[3] R.C. Rodrigues, C. Ortiz, Á. Berenguer-Murcia, R. Torres, R. Fernández-Lafuente, Modifying enzyme activity and selectivity by immobilization, Chem. Soc. Rev. 42 (2013) 6290–307. doi:10.1039/c2cs35231a.

[4] J.M. Goddard, J.H. Hotchkiss, Polymer surface modification for the attachment of bioactive compounds, Prog. Polym. Sci. 32 (2007) 698–725. doi:10.1016/j.progpolymsci.2007.04.002.

[5] S. Cantone, V. Ferrario, L. Corici, C. Ebert, D. Fattor, P. Spizzo, L. Gardossi, Efficient immobilisation of industrial biocatalysts: criteria and constraints for the selection of organic polymeric carriers and immobilisation methods, Chem. Soc. Rev. 42 (2013) 6262–76. doi:10.1039/c3cs35464d.

[6] J.N. Talbert, J.M. Goddard, Enzymes on material surfaces., Colloids Surfaces B Biointerfaces. 93 (2012) 8–

19. doi:10.1016/j.colsurfb.2012.01.003.

[7] C.Z. Dinu, G. Zhu, S.S. Bale, G. Anand, P.J. Reeder, K. Sanford, G. Whited, R.S. Kane, J.S. Dordick, Enzyme-Based Nanoscale Composites for Use as Active Decontamination Surfaces, Adv. Funct. Mater. 20 (2010) 392–398. doi:10.1002/adfm.200901388.

[8] I.P. Rosinha Grundtvig, J.M. Woodley, K. V. Gernaey, A.E. Daugaard, U. Krühne, Shape and topology optimization of enzymatic microreactors, Technical University of Denmark, 2015.

[9] J. Krenková, F. Foret, Immobilized microfluidic enzymatic reactors, Electrophoresis. 25 (2004) 3550–3563. doi:10.1002/elps.200406096.

[10] H. Yamaguchi, T. Honda, M. Miyazaki, Application of enzyme-immobilization technique for microflow reactor, J. Flow Chem. (2016) 1–5. doi:10.1556/1846.2015.00039.

[11] K.F. Jensen, Microchemical systems: Status, challenges, and opportunities, AIChE J. 45 (1999) 2051–2054. doi:10.1002/aic.690451003.

[12] J.W. Swarts, R.C. Kolfschoten, M.C.A.A. Jansen, A.E.M. Janssen, R.M. Boom, Effect of diffusion on enzyme activity in a microreactor, Chem. Eng. J. 162 (2010) 301–306. doi:10.1016/j.cej.2010.04.040.

[13] W. Zhang, S. Lin, C. Wang, J. Hu, C. Li, Z. Zhuang, Y. Zhou, R.A. Mathies, C.J. Yang, PMMA/PDMS valves and pumps for disposable microfluidics., Lab Chip. 9 (2009) 3088–94. doi:10.1039/b907254c.

[14] S.H. Lee, D.H. Kang, H.N. Kim, K.Y. Suh, Use of directly molded poly(methyl methacrylate) channels for microfluidic applications., Lab Chip. 10 (2010) 3300–3306. doi:10.1039/c0lc00127a.

[15] B. Farshchian, S. Park, J. Choi, A. Amirsadeghi, J. Lee, S. Park, 3D nanomolding for lab-on-a-chip applications, Lab Chip. 12 (2012) 4764. doi:10.1039/c2lc40572e.

[16] J.C. McDonald, G.M. Whitesides, Poly(dimethylsiloxane) as a Material for Fabricating Microfluidic Devices, Acc. Chem. Res. 35 (2002) 491–499. doi:10.1021/ac001132d.

[17] G.H. Seong, R.M. Crooks, Efficient mixing and reactions within microfluidic channels using microbead-supported catalysts, J. Am. Chem. Soc. 124 (2002) 13360–13361. doi:10.1021/ja020932y.

[18] G.H. Seong, J. Heo, R.M. Crooks, Measurement of Enzyme Kinetics Using a Continuous-Flow Microfluidic System Measurement of Enzyme Kinetics Using a Continuous-Flow Microfluidic System, Anal. Chem. 75 (2003) 5206–5212. doi:10.1021/ac034155b.

[19] H. Mao, T. Yang, P.S. Cremer, Design and characterization of immobilized enzymes in microfluidic

systems, Anal. Chem. 74 (2002) 379–385. doi:10.1021/ac010822u.

[20] M.A. Holden, S.Y. Jung, P.S. Cremer, Patterning Enzymes Inside Microfluidic Channels via Photoattachment Chemistry, Anal. Chem. 76 (2004) 1838–1843. doi:10.1021/ac035234q.

[21] C.F. Carlborg, T. Haraldsson, K. Öberg, M. Malkoch, W. van der Wijngaart, Beyond PDMS: off-stoichiometry thiol–ene (OSTE) based soft lithography for rapid prototyping of microfluidic devices, Lab Chip. 11 (2011) 3136. doi:10.1039/c1lc20388f.

[22] C.E. Hoyle, C.N. Bowman, Thiol-ene click chemistry., Angew. Chemie. 49 (2010) 1540–1573. doi:10.1002/anie.200903924.

[23] C.F. Carlborg, A. Vastesson, Y. Liu, W. van der Wijngaart, M. Johansson, T. Haraldsson, Functional off-stoichiometry thiol-ene-epoxy thermosets featuring temporally controlled curing stages via an UV/UV dual cure process, J. Polym. Sci. Part A Polym. Chem. 52 (2014) 2604–2615. doi:10.1002/pola.27276.

[24] P. Mazurek, A.E. Daugaard, M. Skolimowski, S. Hvilsted, A.L. Skov, Preparing mono-dispersed liquid core PDMS microcapsules from thiol–ene–epoxy-tailored flow-focusing microfluidic devices, RSC Adv. 5 (2015) 15379–15386. doi:10.1039/C4RA16255B.

[25] T. Haraldsson, C.F. Carlborg, W. van der Wijngaart, OSTE: a novel polymer system developed for Lab-on-Chip, in: Microfluid. BioMEMS, Med. Microsystems XII, 2014. doi:10.1117/12.2041918.

[26] G. Pardon, T. Haraldsson, W. Van Der Wijngaart, Surface energy micropattern inheritance from mold to replica, in: Micro Electro Mech. Syst., 2014: pp. 96–99. doi:10.1109/MEMSYS.2014.6765582.

[27] C.F. Carlborg, F. Moraga, F. Saharil, W. van der Wijngaart, T. Haraldsson, Rapid Permanent Hydrophilic and Hydrophobic Patterning of Polymer Surfaces Via Off-Stoichiometry Thiol-Ene (OSTE) Phtografting, in: Proc. Micro Total Anal. Syst., 2012: pp. 677–679. http://www.rsc.org/images/loc/2012/pdf/M.5.137.pdf.

[28] N.A. Feidenhans'l, J.P. Lafleur, T.G. Jensen, J.P. Kutter, Surface functionalized thiol-ene waveguides for fluorescence biosensing in microfluidic devices, Electrophoresis. 35 (2014) 282–288. doi:10.1002/elps.201300271.

[29] P. Jonkheijm, D. Weinrich, M. Köhn, H. Engelkamp, P.C.M. Christianen, J. Kuhlmann, J.C. Maan, D. Nüsse, H. Schroeder, R. Wacker, R. Breinbauer, C.M. Niemeyer, H. Waldmann, Photochemical Surface Patterning by the Thiol-Ene Reaction, Angew. Chemie. 120 (2008) 4493–4496. doi:10.1002/ange.200800101.

[30] D. Wasserberg, T. Steentjes, M.H.W. Stopel, J. Huskens, C. Blum, V. Subramaniam, P. Jonkheijm, Patterning perylenes on surfaces using thiol–ene chemistry, J. Mater. Chem. 22 (2012) 16606–16610. doi:10.1039/c2jm32610h.

[31] J.P. Lafleur, S. Senkbeil, J. Novotny, G. Nys, N. Bøgelund, K.D. Rand, F. Foret, J.P.J.P. Kutter, Rapid and simple preparation of thiol-ene emulsion-templated monoliths and their application as enzymatic microreactors., Lab Chip. 15 (2015) 1381–1388. doi:10.1039/C4LC01038H.

[32] D. Schäpper, R. Lencastre Fernandes, A.E. Lantz, F. Okkels, H. Bruus, K. V. Gernaey, Topology optimized microbioreactors, Biotechnol. Bioeng. 108 (2011) 786–796. doi:10.1002/bit.23001.

[33] R.H. Ringborg, J.M. Woodley, K. V. Gernaey, U. Krühne, Application of a Microfluidic Tool for the Determination of Enzyme Kinetics, Technical University of Denmark, 2015.

[34] M. Di Fusco, G. Favero, F. Mazzei, Polyazetidine-coated microelectrodes: Electrochemical and diffusion characterization of different redox substrates, J. Phys. Chem. B. 115 (2011) 972–979. doi:10.1021/jp107153c.

[35] M.F. Chaplin, C. Bucke, Enzyme Technology, Cambridge University Press, 1990.

[36] E. Cakmakci, O. Danis, S. Demir, Y. Mulazim, M.V. Kahraman, Alpha-amylase immobilization on epoxy containing thiol-ene photocurable materials, J. Microbiol. Biotechnol. 23 (2013) 205–210. doi:10.4014/jmb.1209.09017.

[37] N. Mogharrab, H. Ghourchian, M. Amininasab, Structural stabilization and functional improvement of horseradish peroxidase upon modification of accessible lysines: experiments and simulation, Biophys. J. 92 (2007) 1192–1203. doi:10.1529/biophysj.106.092858.

[38] N.C. Veitch, Horseradish peroxidase: A modern view of a classic enzyme, Phytochemistry. 65 (2004) 249–259. doi:10.1016/j.phytochem.2003.10.022.

[39] M.M. Bradford, A rapid and sensitive method for the quantitation of microgram quantities of protein utilizing the principle of protein-dye binding, Anal. Biochem. 72 (1976) 248–254. doi:10.1016/0003-2697(76)90527-3.

[40] K.J. Wiechelman, R.D. Braun, J.D. Fitzpatrick, Investigation of the Bicinchoninic Acid Protein Assay: Identification of the Groups Responsible for Color Formation, Anal. Biochem. 237 (1988) 231–237.

[41] B.R.E. Childs, W.G. Bardsley, The Steady-State Kinetics of Peroxidase with 2,2'-Azino-di-(3-

ethylbenzthiazoline- 6-sulphonic acid) as Chromogen, Biochem. J. 145 (1975) 93–103. doi:10.1042/bj1450093.

[42] T.C. Logan, D.S. Clark, T.B. Stachowiak, F. Svec, J.M.J. Fréchet, Photopatterning enzymes on polymer monoliths in microfluidic devices for steady-state kinetic analysis and spatially separated multi-enzyme reactions, Anal. Chem. 79 (2007) 6592–6598. doi:10.1021/ac070705k.

[43] Z. Wang, T.L. King, S.P. Branagan, P.W. Bohn, Enzymatic activity of surface-immobilized horseradish peroxidase confined to micrometer- to nanometer-scale structures in nanocapillary array membranes., Analyst. 134 (2009) 851–859. doi:10.1039/b815590a.

Highlights

Area selective enzyme immobilization and its effect on biocatalytic activity experimentally and by CFD

- Surface patterned OSTE+ microreactor was used to validate effects of enzyme distribution
- The reactor surface was functionalized through stenciled thiol-ene chemistry
- Horseradish peroxidase was immobilized selectively in three surface patterns
- Biocatalytical reactor performance depends greatly on spatial enzyme distribution
- CFD modeling shows good correlation with experimentally observed reactor efficacy